Scientific report; 98 - 01

KNMI

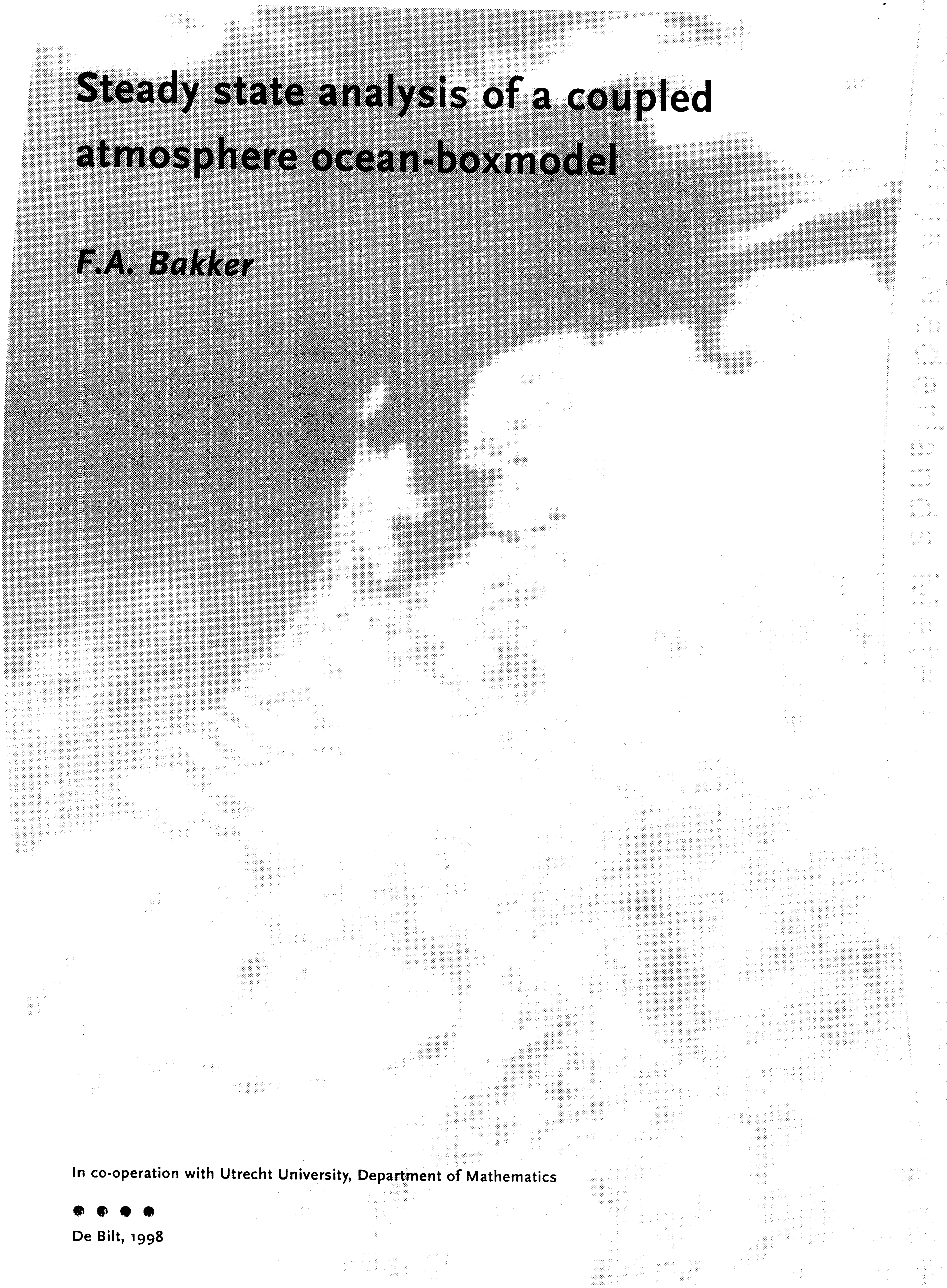

Steady state analysis of a coupled atmosphere ocean-boxmodel

F.A. Bakker

In co-operation with Utrecht University, Department of Mathematics

De Bilt, 1998

Scientific report = wetenschappelijk rapport; WR 98 - 01

De Bilt, 1997

PO Box 201
3730 AE De Bilt
Wilhelminalaan 10
De Bilt
The Netherlands
Telephone + 31(0)30-220 69 11
Telefax + 31 (0)30-221 04 07

Author: F.A. Bakker
Utreecht University, Department of Mathematics

UDC: 551.465.5
551.511
551.526.63

ISSN: 0169-1651

ISBN: 90-369-2133-3

Steady state analysis of a coupled atmosphere ocean-boxmodel

F.A. Bakker

Contents

1. Introduction **3**

2. Model description **3**

2.1 Atmosphere model 3
2.2 Ocean model 3
2.3 Coupled model 4

3. Model analysis **5**

3.1 Equilibrium solutions 5
3.1.1 Relation between T and S at equilibrium *5*
3.1.2 Relation between T, X, G_1 and F_1 at equilibrium *6*
3.1.3 The total solution *7*
3.1.4 Influence of other parameters *7*
3.1.5 F_1-G_1 plane *9*
3.1.6 Stability *10*

4. Conclusions **12**

References **13**

Figure 1: Relation between S and T at equilibrium, with F_1= 0.012. .... *6*
Figure 2: Relation between G_1 and T at equilibrium, with F_1 = 0.012. .... *7*
Figure 3: Maximum and minimum values of F_1 as a function of T. *8*
Figure 4: Generation of an interval without solutions in the G_1-T-curve *9*
Figure 5: Flipping of the small peak in the G_1-T-curve *9*
Figure 6: G_1-F_1 plane with bifurcation curves. *10*
Figure 7: G_1-T-curve with different combinations of eigenvalues, with F_1=0.012 .... *11*
Figure 8: Portions of the G_1-T curve with 4 complex eigenvalues, with F_1=0.012 .... *11*
Figure 9: Stable and unstable portions of the G_1-T-curve, with F_1=0.012 .... *12*

Appendix: G_1 in relation to T, X, S, Y and Z respectively **14**

1. Introduction

In this report the stability behaviour of a coupled atmosphere-ocean model is investigated. The model is a combination of Lorenz's 1984 atmosphere model (Lorenz, 1984) and a simplified version of Stommel's two-box ocean model (Stommel, 1961). It comprises five variables, three describing the atmosphere and two describing the ocean.
The aim of studying this model is to get some insight in the effect of coupling on a chaotic system, and it is hoped that some general properties of coupled models can be found that will also apply to more complex and perhaps more realistic climate models.
The model has been studied before by Gideon Zondervan (Zondervan, 1996) in 1996 by way of numerical experiments. He found some interesting properties. In many cases the behaviour did not differ too much from the original Lorenz-84-model, but in some cases the occurrence of intermittancy was observed. This is the phenomenon that a chaotic regime is from time to time interrupted by an apparently periodic interval. The system will remain in this pseudo-periodic mode for a limited time and then become fully chaotic again.
In the present study the equilibrium solutions of the model and their stability are investigated more closely. This is the first step in a more systematic bifurcation analysis, which may help to understand better some of the results found earlier.

2. Model description

The model is a combination of Lorenz's atmosphere model and a simplified version of Stommel's two-box ocean model. Lorenz's model was chosen because it is one of the simplest atmosphere models that has been shown to exhibit chaotic behaviour, which is considered a vital property of the atmosphere. The ocean model was also chosen for its relative simplicity. The ocean does not generate chaotic behaviour itself but it is driven by the atmosphere, introducing new and longer timescales to the combined model.

2.1 Atmosphere model

The atmosphere model used is Lorenz's 1984 model (Lorenz, 1984). It is described by the following three equations:

$$\dot{X} = -Y^2 - Z^2 + a(F - X) \quad (1)$$
$$\dot{Y} = XY - bXZ - Y + G \quad (2)$$
$$\dot{Z} = bXY + XZ - Z \quad (3)$$

Here X represents the strength of the westerly current, and Y and Z represent the cosine and sine phases of a chain of large superimposed eddies. The parameter F is the forcing of the westerly current by the meridional temperature gradient, and G is the forcing by the continent-ocean temperature contrast. The constants a and b are equal to 0.25 and 4 respectively.

2.2 Ocean model

The ocean model consists of two reservoirs, representing the polar and the equatorial region of the ocean in the northern (or southern) hemisphere. The two boxes are connected by a pipeline at the bottom, and an overflow at the surface. The flow (f) through the pipeline is assumed to be proportional to the temperature (T) and salinity (S) differences. The same amount of water will flow back through the overflow. Thus the exchange of properties between both boxes is independent of the direction of the flow, which is reflected by the use of an absolute value in the equations. The equations used are:

$$\dot{T} = k_a(T_{atm} - T) - |f|T - k_w T \tag{4}$$
$$\dot{S} = \delta - |f|S - k_w S \tag{5}$$
$$f = \omega T - \xi S \tag{6}$$

Herein k_a is a coefficient for the heat exchange between the ocean and the atmosphere, T_{atm} is the temperature difference between polar and equatorial air, k_w is a coefficient for the internal diffusion of the ocean (through the overflow and between the box boundaries), δ represents a constant increase in the salinity difference, through the difference in precipitation and evaporation between the polar and equatorial regions, and ω and ξ are coefficients that account for the different contributions of *T* and *S* to the forcing of the flow.

2.3 Coupled model

Now the two models need to be coupled. Since the strength of the westerly current (*X*) is directly related to the meridional atmospheric temperature gradient (T_{atm}), the latter can be replaced by a function of *X*. In this model a linear relation is assumed.
The water vapour transport (δ) is considered to be the sum of a constant part (δ_0) and a varying part, assumed proportional to the eddy activity (Y^2+Z^2).
Finally the atmospheric forcing parameters *F* and *G* are made relative to the oceanic temperature difference (*T*).
The coupling equations are summarised below:

$$T_{atm} = \gamma X \tag{7}$$
$$\delta = \delta_0 + \delta_1(Y^2 + Z^2) \tag{8}$$
$$F = F_0 + F_1 T \tag{9}$$
$$G = G_0 + G_1(T_{av} - T) \tag{10}$$

The constants k_w, k_a, δ_0, ξ and ω have been chosen according to the estimations made by Roebber (Roebber, 1995) and the coupling parameters F_1, G_1 and δ_1 have been chosen such as to ensure that the atmospheric parameters *F* and *G* are within the "chaotic window" as found by Anastassiades (Anastassiades, 1995). This chaotic window is bounded by $8.0 \leq F \leq 8.5$ and $1.0 \leq G \leq 1.1$. The parameter values thus arrived at are presented in the following table:

a	0.25	b	4.0
F_0	8.0	G_0	1.0
F_1	0.012	G_1	0.010
k_a	1.8*10-4	k_w	1.8*10-5
δ_0	7.8*10-7	δ_1	9.6*10-8
ω	1.3*10-4	ξ	1.1*10-3
T_{av}	30.0	γ	30.0

Table 1: Parameter values

While the other parameters remain constant, F_1 and G_1 are used as bifurcation parameters. In Zondervans experiments they were varied within a window bounded by $0.00 \leq F_1 \leq 0.08$ and $0.00 \leq G_1 \leq 0.08$. In this study we will sometimes extend this region in order to incorporate a region where interesting behaviour occurs. Their default values will be 0.012 and 0.010 respectively.

3. Model analysis

3.1 Equilibrium solutions

The equilibrium solutions of the system are given by the following set of equations:

$$\dot{X} = -Y^2 - Z^2 + a(F_0 + F_1 T - X) = 0 \tag{11}$$

$$\dot{Y} = XY - bXZ - Y + G_0 + G_1(T_{av} - T) = 0 \tag{12}$$

$$\dot{Z} = bXY + XZ - Z = 0 \tag{13}$$

$$\dot{T} = k_a(\gamma X - T) - |\omega T - \xi S| T - k_w T = 0 \tag{14}$$

$$\dot{S} = \delta_0 + \delta_1(Y^2 + Z^2) - |\omega T - \xi S| S - k_w S = 0 \tag{15}$$

The system can be rewritten in the following manner:

$$a\delta_1(k_a + k_w - \gamma k_a F_1)T + \gamma k_a k_w S + (a\delta_1 T + \gamma k_a S)|\omega T - \xi S| - \gamma k_a(\delta_0 + a\delta_1 F_0) = 0 \tag{16}$$

$$X = F_0 + F_1 T + \frac{\delta_0}{a\delta_1} - \frac{1}{a\delta_1}|\omega T - \xi S| S - \frac{k_w}{a\delta_1} S \tag{17}$$

$$a(F_0 + F_1 T - X)(1 - 2X + (1 + b^2)X^2) - (G_0 + G_1(T_{av} - T))^2 = 0 \tag{18}$$

$$Y = \frac{(1 - X)(G_0 + G_1(T_{av} - T))}{1 - 2X + (1 + b^2)X^2} \tag{19}$$

$$Z = \frac{bX(G_0 + G_1(T_{av} - T))}{1 - 2X + (1 + b^2)X^2} \tag{20}$$

3.1.1 Relation between T and S at equilibrium

Expression (16) represents a relation between T and S which must be satisfied in the case of a steady state. In order to simplify the equation the following new constants will be introduced:

$$A = a\delta_1(k_a + k_w - \gamma k_a F_1)$$

$$B = \gamma k_a k_w$$

$$C = a\delta_1$$

$$D = \gamma k_a$$

$$E = \gamma k_a(\delta_0 + a\delta_1 F_0)$$

Herewith expression (16) can be rewritten as:

$$AT + BS + (CT + DS)|\omega T - \xi S| - E = 0 \tag{21}$$

Assuming that ωT-$\xi S \geq 0$ the following two solutions for S are found:

$$S_{1,2} = \frac{1}{2\xi D}(B + (\omega D - \xi C)T) \pm \frac{1}{2\xi D}\sqrt{(B + (\omega D - \xi C)T)^2 + 4\xi D(\omega C T^2 + AT - E)} \tag{22}$$

And assuming that ωT-$\xi S < 0$ two more solutions for S are found:

$$S_{3,4} = -\frac{1}{2\xi D}(B - (\omega D - \xi C)T) \pm \frac{1}{2\xi D}\sqrt{(B - (\omega D - \xi C)T)^2 + 4\xi D(\omega C T^2 - AT + E)} \tag{23}$$

(S_1 and S_3 refer to the equations with the '+'sign, S_2 and S_4 to the equations with the '-'sign.)

In order for these solutions to exist the discriminants must be greater than or equal to zero. For S_1 and S_2 this requires that $T \leq T_a$ or $T \geq T_b$, with T_a and T_b according to:

$$T_{a,b} = -\frac{\omega BD - \xi BC + 2\xi AD \pm \sqrt{(\omega BD - \xi BC + 2\xi AD)^2 - (\omega D + \xi C)^2 (B^2 - 4\xi DE)}}{(\omega D + \xi C)^2} \tag{24}$$

(T_a refers to the equation with the '+'sign, and T_b to the equation with the '-'sign.)
For S_3 and S_4 the discriminant is always positive for the selected parameter ranges.

The solutions S_1 and S_3 intersect the line ωT-$\xi S = 0$ in the point:

$$T_0 = \frac{\xi E}{\omega B + \xi A},\ S_0 = \frac{\omega E}{\omega B + \xi A} \tag{25}$$

Checking the solutions with the assumptions about the sign of ωT-ξS gives us their respective domains:

for $T_b \leq T \leq T_0$ $\qquad S = S_1$ (26)
for $T \geq T_b$ $\qquad S = S_2$ (27)
for $T \leq T_0$ $\qquad S = S_3$ (28)

Solution S_4 doesn't satisfy the assumptions anywhere and must be disregarded.

To complete the description: for the selected parameter range we have that:

for ωT-$\xi S > 0$ $\qquad T \geq T_b > 0$
for ωT-$\xi S < 0$ $\qquad T < T_0,\ S = S_3 > 0$

S_1 and S_2 describe different parts of the same curve, S_3 describes another curve; both curves meet in the point (T_0, S_0).

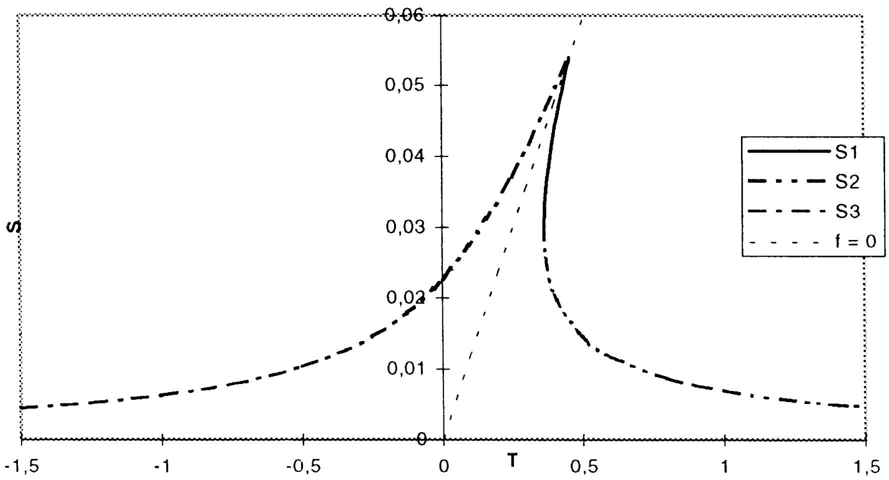

Figure 1: Relation between S and T at equilibrium, with F_1= 0.012.

3.1.2 Relation between T, X, G_1 and F_1 at equilibrium.

Expression (18) gives us a relation between T, X, G_1 en F_1. It is difficult to solve the expression for one of the variables, but it can be solved for the parameter G_1. We find the following two solutions:

$$G_1 = -\frac{G_0}{T_{av} - T} \pm \frac{1}{T_{av} - T}\sqrt{a(F_0 + F_1 T - X)(1 - 2X + (1 + b^2)X^2)} \tag{29}$$

3.1.3 The total solution

Inserting the equations for S_1, S_2 and S_3 into (17) and then inserting the resulting three equations into (29) we find in all six solutions for G_1 as a function of T and F_1. Or three solutions, if we limit ourselves to the positive values of G_1. In a similar manner, which will not be repeated here, an expression for G_1 as a function of X and F_1 can be found. The most striking feature of the curve is the small peak that occurs for $T_b<T<T_0$. In most cases a horizontal line representing a certain constant value of G_1 will intersect the curve one or three times, indicating one or three possible equilibrium solutions, but for one small interval of values of G_1 the horizontal line will also intersect this small peak, raising the number of possible equilibria by two.

Since each of the three solutions for G_1 as a function of T corresponds to only one function S of T, a given combination of G_1 and T will produce only one value of S, and with equations (17), (19) and (20), only one value of X, Y and Z respectively. So we can safely restrict ourselves to the variable T if we wish to find the number of possible equilibria.

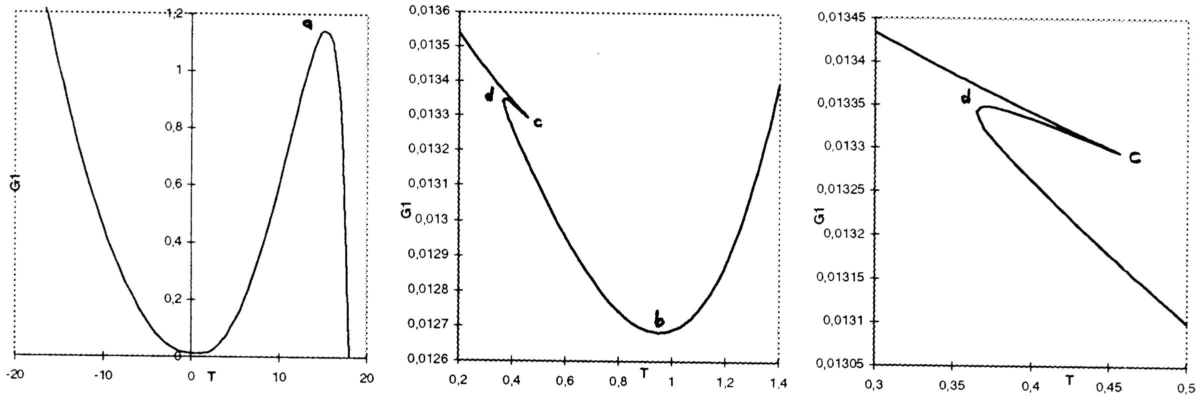

Figure 2: Relation between G_1 and T at equilibrium, with F_1 = 0.012.

3.1.4 Influence of other parameters

Influence of the F_1 parameter

Equation (29) can only be solved if $F_0+F_1T-X \geq 0$. This can be shown to be equivalent with:

$$\delta_0 - |\omega T - \xi S| S - k_w S \leq 0 \tag{30}$$

I. Assuming that $\omega T-\xi S \geq 0$, for S the following inequality is found:

$$\frac{\omega T + k_w - \sqrt{(\omega T + k_w)^2 - 4\xi\delta_0}}{2\xi} \leq S \leq \frac{\omega T + k_w + \sqrt{(\omega T + k_w)^2 - 4\xi\delta_0}}{2\xi} \tag{31}$$

Combining equation (14) with the assumptions that $\omega T-\xi S \geq 0$ and $X \leq F_0+F_1T$ yields:

$$k_a\left(\gamma(F_0 + F_1T) - T\right) - \omega T^2 - k_w T + \xi TS \geq 0 \tag{32}$$

This must be true for even the smallest value of S, which is given by the left-hand side of equation (31):

$$k_a\left(\gamma(F_0 + F_1T) - T\right) - \tfrac{1}{2}T(\omega T + k_w) - \tfrac{1}{2}T\sqrt{(\omega T + k_w)^2 - 4\xi\delta_0} \geq 0 \tag{33}$$

As $\omega T-\xi S \geq 0$ infers that $T > 0$ (see § 3.1.1), we finally find for F_1 the following expression:

$$F_1 \geq -\frac{F_0}{T} + \frac{1}{\gamma} + \frac{1}{2\gamma k_a}\left((\omega T + k_w) + \sqrt{(\omega T + k_w)^2 - 4\xi\delta_0}\right) \tag{34}$$

II. Assuming that ωT-$\xi S < 0$, for S one of the following inequalities must hold:

$$S \leq \frac{\omega T - k_w - \sqrt{(\omega T - k_w)^2 + 4\xi\delta_0}}{2\xi} \tag{35}$$

or

$$S \geq \frac{\omega T - k_w + \sqrt{(\omega T - k_w)^2 + 4\xi\delta_0}}{2\xi} \tag{36}$$

As ωT-$\xi S < 0$ infers that $S > 0$ (see § 3.1.1), expression (35), being always smaller than zero, can be ignored, leaving us only with (36).
Combining equation (14) with the assumptions ωT-$\xi S < 0$ and $X \leq F_0 + F_1 T$ yields:

$$k_a(\gamma(F_0 + F_1 T) - T) + \omega T^2 - k_w T - \xi TS \geq 0 \tag{37}$$

And with (36) we subsequently find:

$$k_a(\gamma(F_0 + F_1 T) - T) + \omega T^2 - k_w T - \tfrac{1}{2}T\left(\omega T - k_w + \sqrt{(\omega T - k_w)^2 + 4\xi\delta_0}\right) \geq 0 \tag{38}$$

For $T < 0$ we find:

$$F_1 \leq -\frac{F_0}{T} + \frac{1}{\gamma} - \frac{1}{2\gamma k_a}\left((\omega T - k_w) - \sqrt{(\omega T - k_w)^2 + 4\xi\delta_0}\right) \tag{39}$$

and for $T > 0$ we find:

$$F_1 \geq -\frac{F_0}{T} + \frac{1}{\gamma} - \frac{1}{2\gamma k_a}\left((\omega T - k_w) - \sqrt{(\omega T - k_w)^2 + 4\xi\delta_0}\right) \tag{40}$$

This last expression yields values of F_1 much smaller than zero, which for the purpose of this study can be ignored, so that for $T > 0$ expression (34), and for $T < 0$ expression (39) will suffice. In the figure below two curves are shown, the area below the left-hand curve corresponding to expression (34) and the area above the right-hand curve to expression (39).

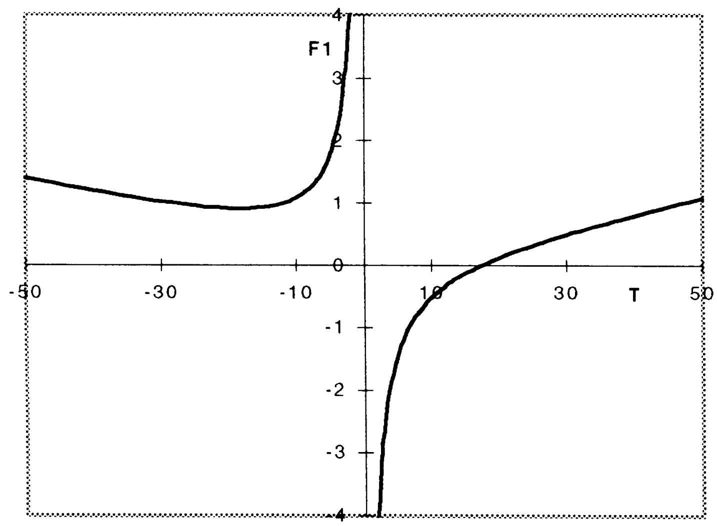

Figure 3: Maximum and minimum values of F_1 as a function of T.

Equilibria are only possible in the area between both curves. Given a certain value of F_1 the intersection with the right-hand curve marks the maximum value of T for which, for a certain G_1, an equilibrium can be found. For values of F_1 greater than 0.92 also two intersections with the left-hand curve occur, marking another interval of T values for which no equilibrium is possible for any value of G_1. The pictures below show the generation of this interval.

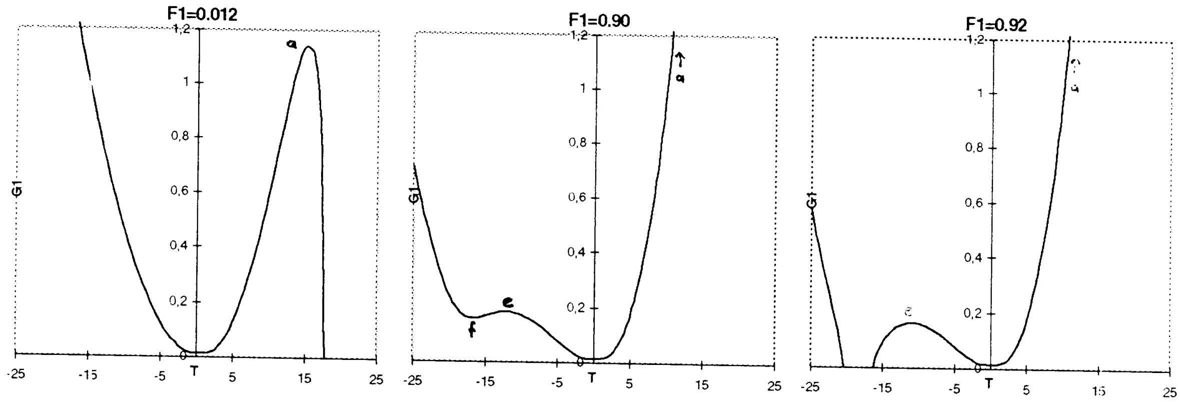

Figure 4: Generation of an interval without solutions in the G_1-T-curve.

In § 3.1.3 the occurrence of a small peak in the G_1-T curve was mentioned. For values of F_1 smaller than about 0.25475 this peak is pointing down, for values of F_1 between 0.25475 and 0.28340 it is horizontal and for F_1 greater than about 0.28340 it is pointing up. This is shown in the figures below:

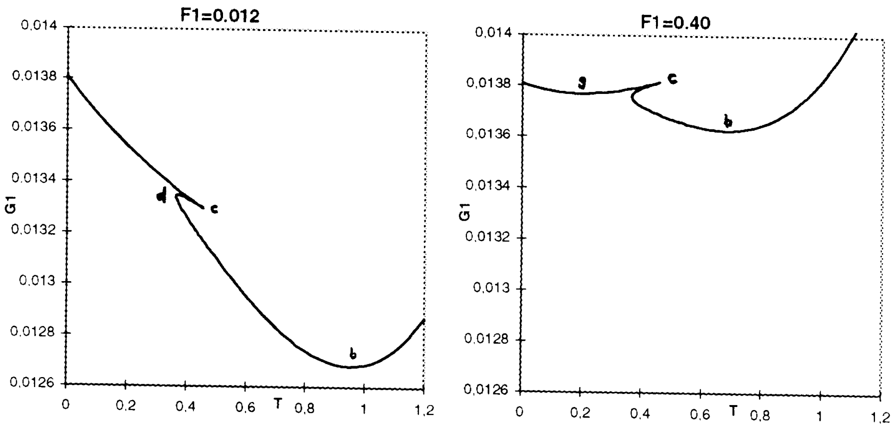

Figure 5: Flipping of the small peak in the G_1-T-curve

Influence of G_0 parameter

If we study equation (29) more closely we find that G_0 only occurs in the first term of the right-hand side and that F_0, F_1, X and T are all independent of G_0. So G_0 only influences G_1 itself. Increasing G_0 will lower G_1 and decreasing G_0 will raise G_1, without significantly changing the characteristic shape of the G_1-T curve.

Influence of F_0 parameter

The influence of F_0 is more complex, as F_0 also determines expressions (34) and (39) and thus the location along the T-axis of several characteristic points. However, the system is not very sensitive to changes in F_0.

3.1.5 F_1-G_1 plane

In the G_1-T curves that have been shown each horizontal tangent, as well as the endpoint of the small peak, represent bifurcations, where two new equilibria appear or disappear when G_1 is changed. The position along the G_1-axis of these bifurcations depends on the value of F_1. In the pictures below part of the F_1-G_1 parameter plane is shown, with curves indicating the different bifurcations. The letters refer to the corresponding bifurcations in the preceding G_1-T plots and the numbers indicate the number of possible equilibrium solutions.

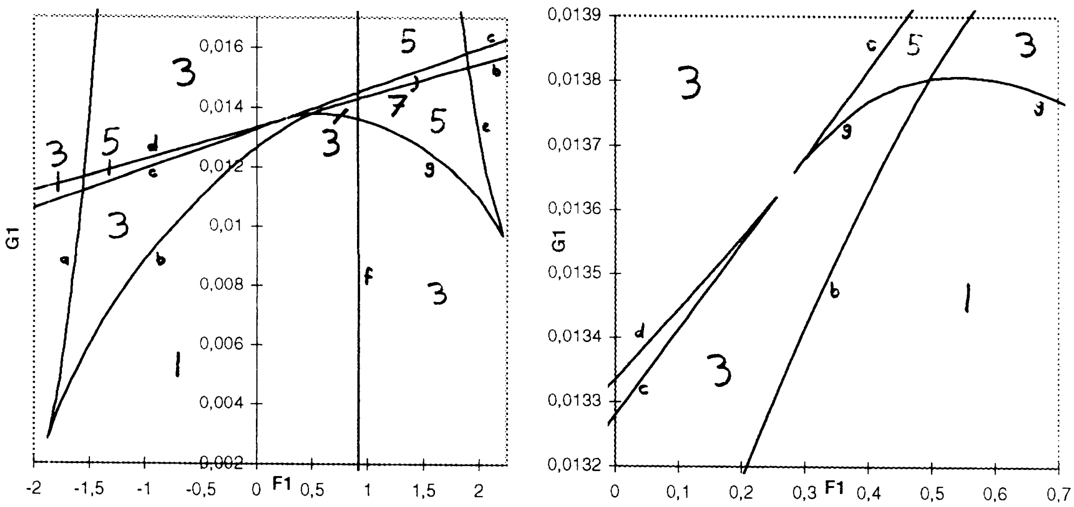

Figure 6: G_1-F_1 plane with bifurcation curves.

3.1.6 Stability

In order to examine the stability of each equilibrium the system will be linearized around an arbitrary steady state. The following Jacobian matrix is found:

$$J = \begin{pmatrix} -a & -2Y & -2Z & aF_1 & 0 \\ Y-bZ & X-1 & -bX & -G_1 & 0 \\ bY+Z & bX & X-1 & 0 & 0 \\ \gamma k_a & 0 & 0 & -\sigma\cdot(2\omega T-\xi S)-k_a-k_w & \sigma\cdot\xi T \\ 0 & 2\delta_1 Y & 2\delta_1 Z & -\sigma\cdot\omega S & -\sigma\cdot(\omega T-2\xi S)-k_w \end{pmatrix} \qquad (41)$$

Here σ denotes the sign of the term $f = \omega T-\xi S$

The eigenvalues of the system follow from $|J-\lambda I| = 0$, where λ denotes the eigenvalues and I the unitary matrix. The equation is of the fifth order in λ and it has 5 roots. The following combinations of eigenvalues are found:

all 5 real parts smaller than zero	
- with 2 complex, both of which are smaller than zero	E522
- with 4 complex, all of which are smaller than zero	E544
with 4 real parts smaller than zero	
- with 2 complex, both of which are smaller than zero	E422
with 3 real parts smaller than zero	
- with 2 complex, none of which are smaller than zero	E320
- with 4 complex, 2 of which are smaller than zero	E342
with 2 real parts smaller than zero	
- with 2 complex, none of which are smaller than zero	E220

In the figure below a G_1-T curve is shown with the different combinations of eigenvalues.

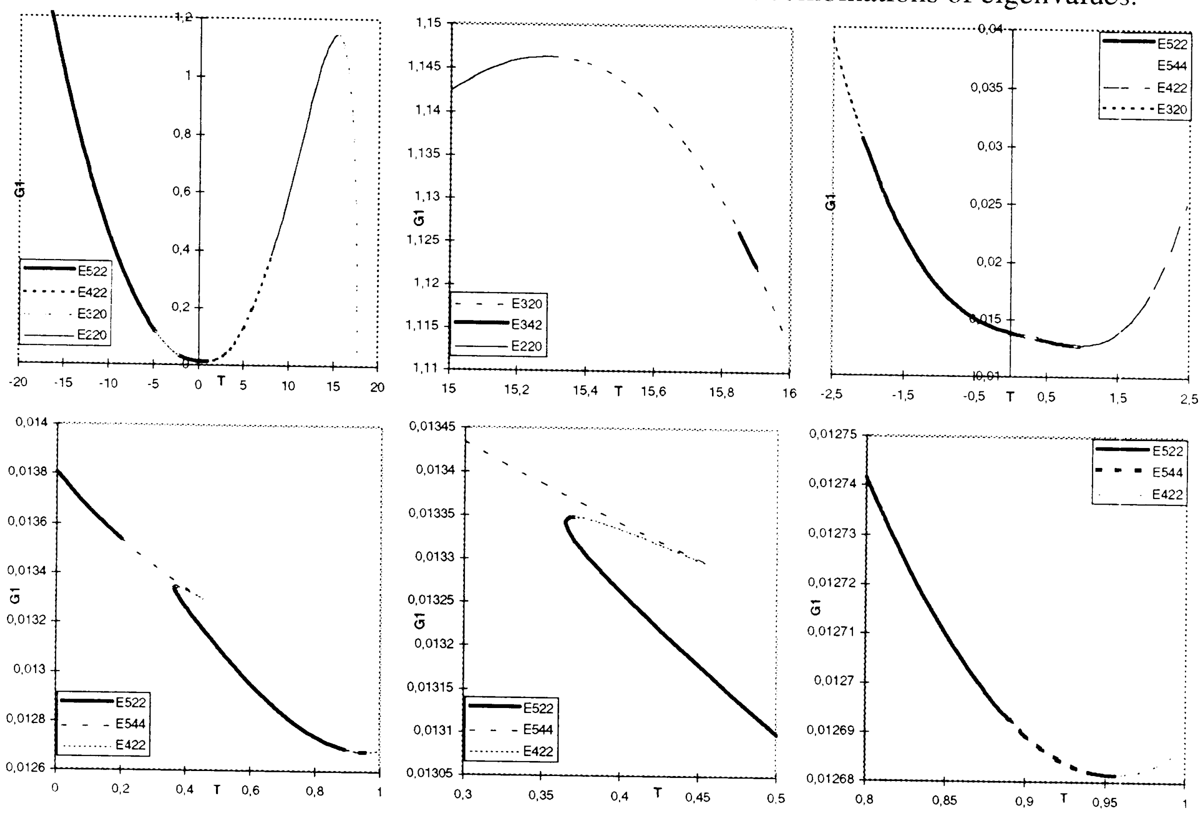

Figure 7: G_1-T-curve with different combinations of eigenvalues, with F_1=0.012

In most cases we find three real eigenvalues and two conjugate complex. This reminds us of the Lorenz-84 model itself where also for each equilibrium one pair of conjugate complex eigenvalues is found (Anastassiades 1995). It is tempting therefore to attribute the occurrence of this complex pair to the atmospheric part of the coupled model. However, there are a few small portions of the G_1-T curve where we find not one but two pairs of complex eigenvalues, as is shown in the picture below.

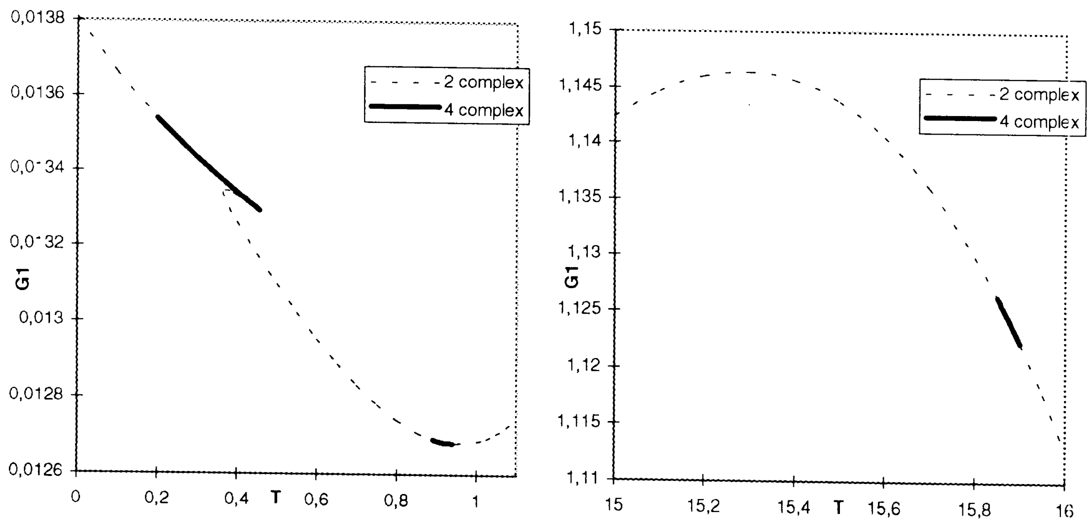

Figure 8: Portions of the G_1-T curve with 4 complex eigenvalues, with F_1=0.012.

Complex eigenvalues are associated with a spiralling movement, outward when the real parts of the eigenvalues are positive, and inward when they are negative. In the case of four complex eigenvalues this spiralling movement must extend to the oceanic variables as well.

Only when the real parts of all five eigenvalues are smaller than zero, the equilibrium is stable. In the figures below the G_1-T curve for F_1=0.012 is shown again and the stable and unstable regions are indicated.

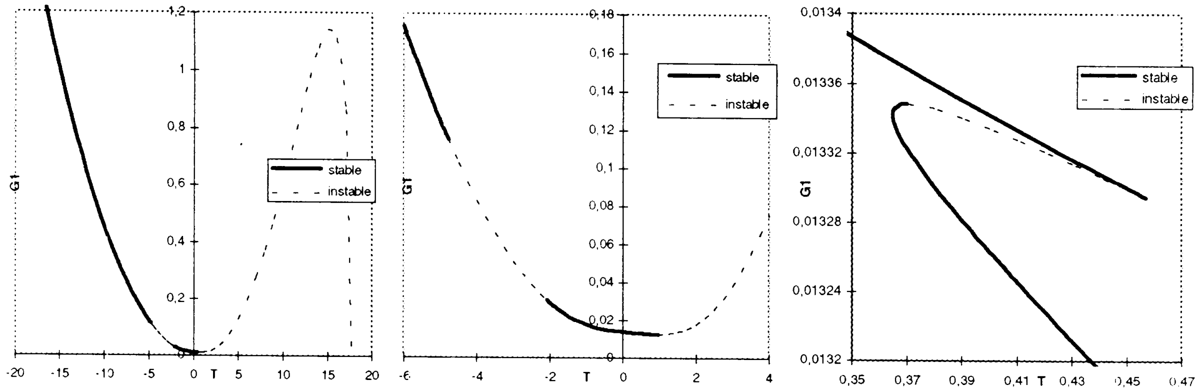

Figure 9: Stable and unstable portions of the G_1-T-curve, with F_1=0.012.

Three stable regions can be discerned. The first covers all values of G_1 > 0.11326 and $T > -4.79$, the second region covers all values of G_1 from 0.03044 down to 0.013294, where the peak occurs, and T from -2.08 up to +0.4568, and the third region all values of G_1 from 0.013348 down to 0.0126821, and T from 0.3645 up to 0.9563. The second and third stable regions have a small overlap, as can be seen in the third picture. On the edge of the peak the eigenvalues are undetermined.

4. Conclusions

It is not possible to express the equilibrium solutions explicitly as functions of the two bifurcation parameters. We can, however, express G_1 as a function of T and F_1, while the other four variables can be expressed explicitly as functions of G_1, F_1 and T.
The number and positions of the equilibria do not seem to be very sensitive to changes in F_1. They are, however, quite sensitive to changes in G_1. The curve representing the relation between G_1 and T exhibits a small 'peak', a small fold, where three equilibrium solutions come close together, ending in a sharp edge, where the flow between both ocean boxes is zero.
Within the specified ranges of F_1 and G_1 we find 1 or 3 possible solutions, or even 5, when the small 'peak' is intersected. Of these equilibria 0, 1 or 2 are found to be stable. Although along the peak two stable equilibria are found to exist, they appear to have extremely small regions of attraction making it very hard to find them numerically.
For almost all equilibria we find three real and two conjugate complex eigenvalues. The latter may very well be attributed to the atmospheric part of the model, since the equilibrium solutions of the Lorenz-84 model themselves always exhibit two complex eigenvalues. However, in some small regions we find not one but two pairs of conjugate complex eigenvalues, so that the ocean must be implicated as well.

Several questions remain, that will have to be answered in a continued investigation: What is the physical meaning of the peak? What influence does the peak have on periodic or chaotic solutions nearby? What is the meaning of the occurrence of a second pair of conjugate complex eigenvalues? How do the variables converge to or diverge from such an equilibrium?

References

[1] Anastassiades, L., 1995: Numerical studies on the Lorenz-84 atmosphere model, KNMI WR 95-05.

[2] Lorenz, E.N., 1984: Irregularity: a fundamental property of the atmosphere, Tellus 36A, p. 98-110.

[3] Roebber, P.J., 1995: Climate variability in a low order coupled atmosphere model, Tellus 47A, p. 473-494.

[4] Stommel, H., 1961: Thermohaline convection with two stable regimes of flow, Tellus 13, p. 224-230.

[5] Zondervan, G., 1996: Chaos and coupling: a coupled atmosphere ocean-boxmodel for coupled behaviour studies, KNMI WR 96-02.

Appendix: G_1 in relation to T, X, S, Y and Z respectively.